Available online at www.sciencedirect.com
SCIENCE DIRECT®
Journal of Sound and Vibration 276 (2004) 541–570
JOURNAL OF SOUND AND VIBRATION
www.elsevier.com/locate/jsvi

Wave attenuation in periodic three-layered beams: analytical and FEM study

Venkata Mangaraju, Venkata R. Sonti*

Facility for Research in Technical Acoustics, Department of Mechanical Engineering, Indian Institute of Science, Bangalore 560012, India

Received 30 September 2002; accepted 4 August 2003

Abstract

We study infinite composite beams with periodic simple supports and analyze their vibration attenuation characteristics. In the literature single spans of such beams have been studied for determining their loss factors. Such loss factor information is insufficient for determining attenuation in the periodic or multi-span case. Here, we directly derive propagation constants as a function of frequency. Two distinct cases are investigated in detail. The first is a three-layered periodic beam with a continuous central visco-elastic layer. The second is a periodic beam with visco-elastic inserts of finite extent. The former is analytically tractable and yields insight, while the latter has better structural properties for practical applications. The continuous layer case is studied using several different beam theories. The case with inserts is studied for several different configurations using FEM. Dependence of attenuation characteristics on size, location, and number of inserts is presented. This study provides insights that will be useful for designing visco-elastic inserts for vibration attenuation in periodic structures.

1. Introduction

Vibrations from sources such as engines are transmitted to distant parts of the system by beam type supporting structures in the form of various waves (flexural, torsional, and longitudinal). These waves interfere with the functioning of other sub-systems and even radiate as sound. A typical example is a ship structure, where the engine is mounted on a foundation which is in the form of a periodic grillage of beams (or the hull which is a periodic construction of beams and

*Corresponding author. Tel.: +91-80-309-2671.
E-mail address: sonti@mecheng.iisc.ernet.in (V.R. Sonti).

0022-460X/$ - see front matter © 2003 Elsevier Ltd. All rights reserved.
doi:10.1016/j.jsv.2003.08.033

plates). This grillage transmits engine vibrations to the sonar compartment, to the residential cabins, and finally to the hull and to the outside as sound. The excitation is both periodic and random, covering a broad range of frequencies. Discontinuities in various forms such as masses, cross beam structures and changes in material do cause reflections and reduce the transmitted energy, yet the degree of attenuation is insufficient, inadequate over a broad range of frequencies and the regions between these discontinuities exhibit local resonances. The inadequacy comes because the attenuation occurs only due to the reflections at the junctions or discontinuities and not throughout the vibration propagation path.

These foundation structures are typically modelled as periodic structures (periodic implies infinite structures with a certain periodicity). Such systems have been studied for nearly 300 years as pointed out by Brillouin in his classic work [1]. Physicists and electrical engineers have developed the studies over the years in relation to crystals, optics, electrical transmission lines, etc. It is only in recent times that wave motion in engineering periodic structures (consisting of beams, plates, etc.) has been investigated. These periodic structures lend themselves to analysis using wave propagation methods.

A significant amount of research material exists in the area of periodic structures. One such typical structure is the periodically supported beam [2]. In this structure, typically, a damping layer is added to attenuate vibrations. Such a layer damps vibrations throughout the wave propagation path and not just at junctions. However, these studies have mainly investigated loss factors. Studies on layered periodic beams for understanding wave propagation have not been done in much detail. Since the area has been researched for a long time, it is only proper that we present a brief yet sufficient review of the relevant literature.

Sen Gupta [3] used a graphical network to determine the natural frequencies of flexural vibration of continuous beams having any number of spans of uniform length. Narrow attenuation zones and amplification zones in finite and semi-infinite beams were analyzed. Cremer and Leilich [4] studied flexural motion in periodic beam structures, and showed that waves propagate in some frequency bands but not in others. Ellington and McCallion [5] studied the free vibration of grillages on the assumption that the mass of the beams is concentrated at the nodes and that the beams do not resist torsion. The effect of the approximation inherent in the lumping of masses was also investigated. Thein Wah's [6] investigation revealed that at least for the case of the simple support on all edges of the grillage, the lowest natural frequencies were closely approximated by the lumped-mass approximation. Thein Wah [7] also investigated the free oscillations of a uniform grillage using finite difference calculus technique. The theory is approximate in that the mass of the beams is concentrated at the nodes. Solutions for a simply supported grillage were developed.

Heckl [8] studied the vibration of a grillage using Euler Beam Theory and wave approach. He demonstrated the same property that waves can propagate in some frequency bands but not in others. In general it was found that out of the several propagation constants, that with the least attenuation carries all the waves to the far field. Yong and Lin in Refs. [9,10] developed time domain methods for planar and three dimensional (3-D) truss type structures. In Ref. [10] a 3-D truss with a complex looped configuration was investigated to form the basic unit which was repeated to form the full structure. Once the basic unit is formed this essentially is a 1-D formulation. Similar work was presented by Flotow [11] for a complex structural network of beams and rods. System impulse responses were investigated.

Roy and Plunkett [12] investigated wave attenuation in infinite periodic beams with cross ribs. Both analysis and experiments using a limited number of ribs were done. The results were presented in terms of insertion loss. Kerwin [13], and Saito and Sato [14] investigated damping of flexural waves in beams using a constrained layer. Kerwin presented analytical and experimental results for loss factors. Saito and Sato presented a 2-D elasticity view point followed by a study of the dispersion relation for the three-layered beam as a function of frequency. In the paper [15], the sixth order differential equation of motion for a three-layered sandwich beam with a visco-elastic core was derived in terms of the transverse displacement (η). Mathematical expressions in terms of η were found for a variety of boundary conditions. The solution of the differential equation was shown to yield a special class of complex, forced modes of vibration which were completely uncoupled.

Mead and his co-workers [16,17] included the effects of damping in the wave propagation theory for periodic beams, and later discussed the nature of the propagating waves and their possible interaction with acoustic waves. In the paper [16], a three-layered encastre sandwich beam was investigated and its characteristic equation for the resonant frequency, loss factor and modal roots were determined. A method for general boundary conditions was presented. In this context, Reddy and Mallik [18,19] studied the natural frequencies and modal loss factors of two and three-layered periodic rings, respectively.

This was followed by a study of the harmonic and random responses of periodic beams on elastic supports and subjected to loading [20,21]. In the paper [20], the relationship between the bounding frequencies of the propagation zones of mono-coupled periodic systems and the natural frequencies of the individual elements of which the system is composed was studied. The concept of characteristic receptance was derived. In Ref. [21] a general theory in 1-D systems with multiple coupling between adjacent elements was presented. The nature and number of different wave propagation constants was discussed. It was then shown that all equations so derived for free undamped wave motion were applicable to the damped forced motion of hysteretically damped multi-coupled systems. Loss factors were investigated and finite periodic systems of damped multi-coupled elements were finally studied.

Sen Gupta [22] studied the rib skin periodic structure by wave propagation methods and showed how natural frequencies of finite beam type periodic structures can be found from wave propagation characteristics. Flexural propagation constants were determined for a continuous infinite beam (periodically supported) with rigid supports and also flexible supports. Euler Beam Theory and Receptance approach were used to find propagation constants. It was found that a beam on rigid supports has a single wave propagation constant for each frequency and a single well-defined free wave group. A beam on flexible supports has two propagation constants for each frequency, and two corresponding free wave groups.

Miller and Flotow [23] investigated the dynamics of homogenous beam networks using Euler beam theory. He and Rao [24], presented an analytical model for the study of coupled transverse and longitudinal vibration of multi-span sandwich beam systems with arbitrary boundary conditions. In this paper only modes and loss factors were investigated.

Mace [25] developed a new three-layered beam element with a central visco-elastic layer to be used in FEM and compared the response and natural frequencies using standard packages. In the paper [26], a three-layered beam theory was given in which the continuity of displacements and transverse shear stresses was satisfied at the interfaces. Axial displacement field in each layer was

assumed to be non-linear with respect to the thickness co-ordinate. This proposed sandwich beam theory was used to predict loss factors of visco-elastically damped simply supported beams. Bondaryk [27] conducted experimental measurements to understand the behaviour of trusses in the frequency range 10–1400 Hz.

Fasana and Marchesiello [28] have also recently investigated modal frequencies of finite sandwich beams with various boundary conditions. Polynomials were used as admissible functions, leading to simple expressions for energy integrals. Xu and Huang [29] investigated vibration reduction in a multi-span beam using a random wave reflector method. They introduced different wave carrying media into the beam in a random sequence. The uncorrelated nature of the reflections from different interfaces caused a general amplification in propagation constants.

Thus, it may be seen that the damping-related literature on periodic structures deals mostly with loss factors and/or natural frequencies, which relate to a single span of the periodic structure. The relationship between the loss factor and the attenuation at a certain frequency in a periodic structure is not obvious. It has to be found. We have addressed this issue by determining the actual propagation constant curve which includes the damping effect of the visco-elastic layer.

In this paper, the work presented is partitioned into *two distinct* sections. In the *first section*, (Part I) a detailed analytical derivation of wave propagation in a three-layered periodically supported infinite beam is presented. Of the three layers, the central layer is visco-elastic and damps out vibrations as they propagate through the structure. An analytical model is developed based on Timoshenko theory [32]. Then, propagation constants are computed and compared with those of a homogenous periodically supported beam [2] (see Fig. 1). The similarities and differences are investigated in detail using several intermediate equivalent theories.

In the *second section* (Part II), the three-layered infinite periodically supported beam mentioned above is modelled in FEM and its vibration attenuation characteristics analyzed. In the analytical study (Part I), the model is limited by Timoshenko theory restrictions [2] and not only that, the central visco-elastic layer is placed throughout the periodic beam. This is convenient for using analytical wave propagation methods. However, in practice, a soft damping layer placed throughout has a weakening effect on the structure. It is better to place it at strategic locations in the form of inserts, thereby damping the vibrations and at the same time maintaining the strength of the structure. But again, such an insert configuration does not lend itself easily to wave propagation methods. A numerical approach is needed. Part II uses finite element method (FEM) to model the periodic beam with visco-elastic inserts.

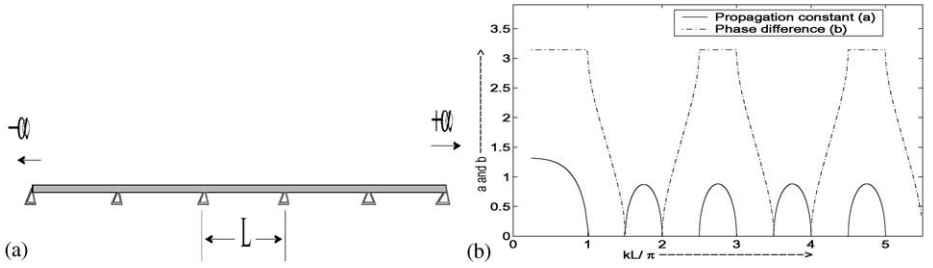

Fig. 1. (a) Sketch of infinite periodic beam. (b) Variation of propagation constant '*a*' and phase coefficient '*b*' for Euler theory as a function of non-dimensional frequency kL in a periodic homogeneous beam.

The FEM study is performed in ANSYS by initially obtaining comparable results with the three-layered analytical model with the continuous visco-elastic layer. This is done not so much to verify FEM against analytical study (ANSYS is a time-tested package) but to establish the place, accuracies and advantages/limitations of one over the other. (It is already known that the analytical model is governed by Timoshenko theory restrictions.) And to be comfortable that we are using the B2D and S73 elements as they should be. By knowing the differences in the results and by accounting for them approximately we establish confidence in the way the package is used. This comparison does clarify certain issues as discussed later. Then, within FEM certain internal consistencies are established in a non-rigorous manner.

After this is done, several studies are performed using the ANSYS package. An approximate equation is derived which non-dimensionalizes the propagation constants so that given a starting configuration, the propagation constant for any other given configuration can be obtained from this equation, with less computations. Next, FEM is used in studying visco-elastic insert configurations.

2. Part I: analytical method

2.1. Wave propagation in an infinite periodic three-layered beam

2.1.1. Three-layered beam theory

Consider a three-layered beam [32] with densities ϱ_1, ϱ_2, ϱ_3, Young's moduli E_1, E_2, E_3, and shear moduli G_1, G_2, G_3. The three thicknesses are d_1, d_2, d_3, respectively, and the width of the beam is b (see Fig. 2). Each of the layers in the beam is allowed to have independent shear strain in accordance with Timoshenko Beam Theory [2,30] and independent rotation due to flexure. However, the slope of the beam is the same at a given x location in the beam. Each layer has its independent axial deformation in its horizontal plane but, transverse motion in the y direction is common to all. As can be seen from Fig. 2, the in-plane displacement (longitudinal displacements)

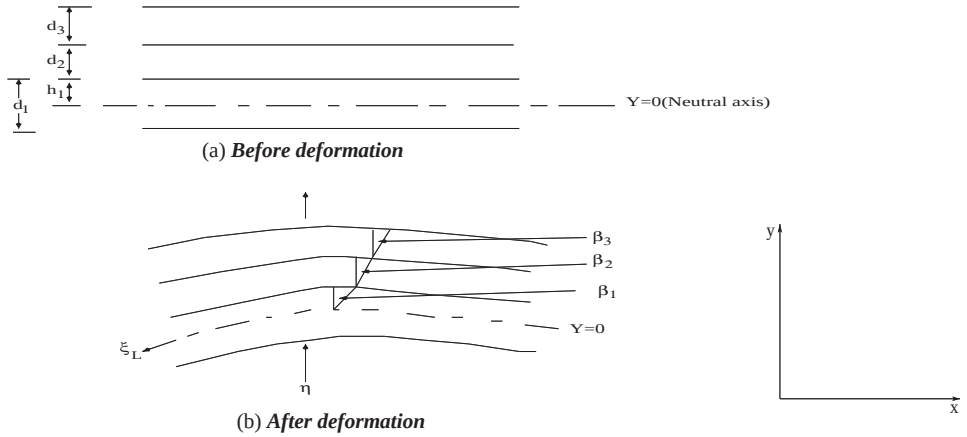

Fig. 2. Displacements and rotations in a three-layered beam.

in the three layers are given by

$$\xi_1 = \xi_L + y\beta_1, \tag{1}$$

$$\xi_2 = \xi_L + h_1\beta_1 + (y - h_1)\beta_2, \tag{2}$$

$$\xi_3 = \xi_L + h_1\beta_1 + d_2\beta_2 + (y - h_1 - d_2)\beta_3, \tag{3}$$

where ξ_L is the longitudinal displacement of the neutral axis of the beam. The displacement in the transverse y direction is η which is assumed to be independent of y. β_1, β_2, β_3 are the rotations due to flexure in the three layers respectively. The reference plane $y = 0$ is arbitrary. Its position has no effect on the final results.

The longitudinal strains are given by

$$\varepsilon_1 = \frac{\mathrm{d}\xi_1}{\mathrm{d}x} = \xi'_L + y\beta'_1, \tag{4}$$

$$\varepsilon_2 = \frac{\mathrm{d}\xi_2}{\mathrm{d}x} = \xi'_L + h_1\beta'_1 + (y - h_1)\beta'_2, \tag{5}$$

$$\varepsilon_3 = \frac{\mathrm{d}\xi_3}{\mathrm{d}x} = \xi'_L + h_1\beta'_1 + d_2\beta'_2 + (y - h_1 - d_2)\beta'_3, \tag{6}$$

where ε_1 is the longitudinal strain in the layer of thickness d_1, ε_2 is the longitudinal strain in the layer of thickness d_2 and ε_3 is the longitudinal strain in the layer of thickness d_3. The shear strain are given by

$$\gamma_i = \frac{\mathrm{d}\xi_i}{\mathrm{d}y} + \frac{\mathrm{d}\eta}{\mathrm{d}x} = \beta_i + \eta', \quad i = 1, 2, 3, \tag{7}$$

where γ_i is the shear strain in the layer of thickness d_i. The prime denotes a derivative with respect to x. The total kinetic energy of the beam is given by [32]

$$E_{kin} = \frac{b}{2}\int_{-l}^{l}\left(\sum_i \int_{d_{li}}^{d_{ui}} \varrho_i(\dot{\xi}_i^2 + \dot{\eta}^2)\,\mathrm{d}y\right)\mathrm{d}x, \quad i = 1, 2, 3 \tag{8}$$

and the total potential energy of the beam is given by

$$E_{pot} = \frac{b}{2}\int_{-l}^{l}\left(\sum i \int_{d_{li}}^{d_{ui}} (E_i\varepsilon_i^2 + G_1\gamma_i^2)\,\mathrm{d}y\right)\mathrm{d}x, \quad i = 1, 2, 3. \tag{9}$$

In the above equations, i denotes the particular layer and d_{li} and d_{ui}, denote the appropriate lower and upper co-ordinates of the ith layer. Next, we apply Hamilton's principle, to obtain a set of partial differential equations for ξ_L, η, β_1, β_2, β_3 and natural boundary conditions. The partial differential equations are given below:

$$\varphi''_1 + \ddot{\varphi}_1 = 0, \quad \varphi''_2 + \ddot{\varphi}_2 = 0, \quad \varphi''_3 + \ddot{\varphi}_3 = 0, \quad \varphi''_4 + \ddot{\varphi}_4 = 0, \quad \varphi''_5 + \ddot{\varphi}_5 = 0, \tag{10}$$

where the variables in Eq. (10) are given in Appendix A. In these equations double dash represent second derivative with respect to space (x) and double dot represent second derivative with respect to time. If we next assume that all motions consist of plane waves of the type

$$A = A_0 \mathrm{e}^{\mathrm{j}(\omega t - kx)},$$

where A denotes displacement or rotation, then substituting the above relations into the five partial differential equations (10) we get the following dispersion relation:

$$\begin{bmatrix} \Omega_{11} & \Omega_{12} & \Omega_{13} & \Omega_{14} & \Omega_{15} \\ \Omega_{21} & \Omega_{22} & \Omega_{23} & \Omega_{24} & \Omega_{25} \\ \Omega_{31} & \Omega_{32} & \Omega_{33} & \Omega_{34} & \Omega_{35} \\ \Omega_{41} & \Omega_{42} & \Omega_{43} & \Omega_{44} & \Omega_{45} \\ \Omega_{51} & \Omega_{52} & \Omega_{53} & \Omega_{54} & \Omega_{55} \end{bmatrix} \begin{bmatrix} \xi_L \\ \eta \\ \beta_1 \\ \beta_2 \\ \beta_3 \end{bmatrix} = \begin{bmatrix} 0 \\ q_0 \\ 0 \\ 0 \\ 0 \end{bmatrix}. \tag{11}$$

The elements of the coefficient matrix in Eq. (11) are given in Appendix B. The variable q_0 is the driving amplitude in units of pressure. The natural boundary conditions obtained from Hamilton's principle are (at $x = -L$ and L)

$$\eta = 0 \text{ or } F_s = 0, \quad \beta_i = 0 \text{ or } M_i = 0 \quad (i = 1,2,3), \quad \xi_1 = 0 \text{ or } F_l = 0,$$

where the shear force and the moment expression details are given in Appendix C.

The three types of motion, longitudinal, shear and bending are coupled with each other. If the layer configuration does not have a plane of symmetry there is no way of decoupling the motions for all frequencies. The zeros of the determinant of the coefficient matrix in Eq. (11) give the free wavenumbers. If E_1, G_1, E_2, G_2 and E_3, G_3 are assumed complex, then the imaginary part of the wavenumber gives the decay constant or the loss factor. It turns out that there are five different free wavenumbers for each frequency, but in the frequency range of interest only two of them are real and so correspond to propagating waves. Of the two propagating wavenumbers, one is related to flexure and the other to the longitudinal wave. If we neglect the longitudinal wave (i.e., drop ξ_L), which has been found to be a valid assumption in the frequency ranges of interest, then the first row and the first column in the coefficient matrix of Eq. (11) can be dropped. The coefficient matrix is now of order 4. Next, we can find β_1, β_2, β_3 in terms of η, which are essential for finding wave reflection and transmission coefficients. The relations among the remaining four variables can be given as follows:

$$\begin{aligned} \frac{\beta_1}{\eta} &= -\frac{c_{12}}{c_{13}}, \\ \frac{\beta_2}{\eta} &= \frac{-(\Omega_{32}\Omega_{25} - \Omega_{22}\Omega_{35})}{c_{11}} - \left(\left(\frac{\beta_1}{\eta}\right)\left(\frac{\Omega_{33}\Omega_{25} - \Omega_{23}\Omega_{35})}{c_{11}}\right)\right), \\ \frac{\beta_3}{\eta} &= \left(\frac{-1}{\Omega_{25}}\right)\left(\Omega_{22} + \Omega_{23}\frac{\beta_1}{\eta} + \Omega_{24}\frac{\beta_2}{\eta}\right), \end{aligned} \tag{12}$$

where

$$\begin{aligned} c_{11} &= \Omega_{25}\Omega_{34} - \Omega_{35}\Omega_{24}, \\ c_{12} &= \Omega_{42} - \Omega_{44}\frac{(\Omega_{32}\Omega_{25} - \Omega_{22}\Omega_{35})}{c_{11}} - \left(\frac{\Omega_{45}}{\Omega_{25}}\right)\left(\Omega_{22} - \Omega_{24}\frac{(\Omega_{32}\Omega_{25} - \Omega_{22}\Omega_{35})}{c_{11}}\right), \\ c_{13} &= \Omega_{43} - \Omega_{44}\frac{(\Omega_{33}\Omega_{25} - \Omega_{23}\Omega_{35})}{c_{11}} - \left(\frac{\Omega_{45}}{\Omega_{25}}\right)\left(\Omega_{23} - \Omega_{24}\frac{(\Omega_{33}\Omega_{25} - \Omega_{23}\Omega_{35})}{c_{11}}\right). \end{aligned}$$

Thus, in any three-layered section carrying a flexural wave, there will be four variables $(\eta, \beta_1, \beta_2, \beta_3)$ each depending on four wavenumbers and hence four coefficients. Thus, there appear to be 16 unknowns. However, at every wavenumber, the four variables are related by Eq. (12). Hence, in any section the unknowns are finally four.

2.1.2. Wave propagation in a periodic three-layered beam with visco-elastic layer

In this section, the set of equations for obtaining the propagation constants for an infinite periodically supported three-layered beam are presented. In the previous section we had found that the three-layered model gives five wavenumbers. Of this, two are real (flexural and longitudinal) and three are imaginary. The longitudinal wavenumber is neglected in this analytical study. In a companion study, FEM modelling has proved the validity of this assumption.

The calculation is presented in two steps. In the first step, the transmission and reflection coefficients for a single support in an infinite three-layered beam subjected to an incident flexural wave are obtained. This derivation is related to Fig. 3a. These coefficients are used in the second step to obtain the propagation constant, the relevant figure for which is Fig. 3b.

Fig. 3a shows an infinite three-layered beam with a single support at $x = 0$ which divides the beam into two sections, section 1 and section 2. Let a wave be incident on the support from section 1 with magnitude given by

$$(v_0 e^{-jk_1 x})e^{j\omega t} \quad \text{for } (x \leqslant 0).$$

The total wave in section 1 is the sum of the incident and reflected waves

$$v_1 = (v_0 e^{-jk_1 x} + re^{jk_1 x} + A_1 e^{jk_2 x} + A_2 e^{jk_3 x} + A_3 e^{jk_4 x})e^{j\omega t} \quad \text{for } (x \leqslant 0). \tag{13}$$

Similarly, the total wave in section 2 is

$$v_2 = (te^{-jk_1 x} + A_4 e^{-jk_2 x} + A_5 e^{-jk_3 x} + A_6 e^{-jk_4 x})e^{j\omega t} \quad \text{for } (x \geqslant 0). \tag{14}$$

In the above equations, r and t are the reflection and transmission coefficients of the support respectively. The wavenumbers k_1, k_2, k_3, k_4 are general wavenumbers. However, for Timoshenko theory only one wavenumber k_1 is propagating which is used below. Since only relative magnitudes of waves are needed v_0 is assumed to be 1. We have eight unknowns (r, t and A_1 to A_6)

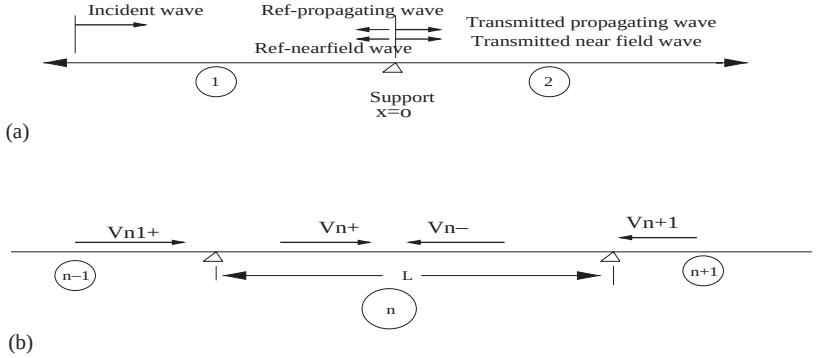

Fig. 3. (a) A single support in an infinite beam. (b) nth span in a periodic beam.

for which the required eight equations are

$$v_1 = 0, \quad v_1 = v_2, \quad \beta_{11} = \beta_{21}, \quad \beta_{12} = \beta_{22}, \quad \beta_{13} = \beta_{23},$$
$$M_{11} = M_{21}, \quad M_{12} = M_{22}, \quad M_{13} = M_{23}. \tag{15}$$

In Eq. (15), the first letter in the subscript represents the section number and the second letter represents the layer number. The details of the expression are given in Appendix C. Using the above derivation we can find reflection and transmission coefficients at the support.

Next, with reference to Fig. 3b (which shows the $n-1$, n and $n+1$th spans in a three-layered periodic beam), the velocity v in each of the sections (denoted by n) is the sum total of infinite reflections of waves propagating within the section n after initially being transmitted into it due to flexure in the neighbouring sections. These summed velocities for a particular section n are denoted by v_n^+ and v_n^-. The '+' sign indicates a right travelling wave and '−' denotes a left travelling wave.

Let us consider the section n in Fig. 3b. The waves from the neighbouring sections contributing to v_n^+ which is a wave travelling to the right are (1) the transmitted component of v_{n-1}^+, (2) the right travelling component due to v_{n+1}^- (initially transmitted into section n) then after one reflection at the left support of the section (n). These two contributions will go through infinite reflections within the section n. The reflections form an infinite geometric series and hence are summed up accordingly. After considering all these waves the equation for v_n^+ is given by

$$v_n^+ = n_x(v_{n-1}^+ t\mathrm{e}^{-\mathrm{i}k_1 L} + v_{n+1}^- tr\mathrm{e}^{-2\mathrm{i}k_1 L}), \tag{16}$$

where

$$n_x = \frac{1}{(1 - r^2\mathrm{e}^{(-2\mathrm{i}k_1 L)})}.$$

Similarly for the wave v_n^- there will be two contributions from the neighbouring sections. The equation is similar to Eq. (16). And since the structure is periodic, we assume

$$\frac{v_{n-1^+}}{v_{n^+}} = \frac{v_{n^-}}{v_{n+1}^-} = \mathrm{e}^g.$$

After substitution of the above relation into Eq. (16) for v_n^+ and a similar equation for v_n^-, we can write

$$v_{n^+}(n_x t\mathrm{e}^{(-\mathrm{i}k_1 L)}\mathrm{e}^g - 1) + v_{n^-}\left(n_x tr\mathrm{e}^{(-2\mathrm{i}k_1 L)}\frac{1}{\mathrm{e}^g}\right) = 0,$$
$$v_{n^-}\left(n_x t\mathrm{e}^{(-\mathrm{i}k_1 L)}\frac{1}{\mathrm{e}^g} - 1\right) + v_{n^+}(n_x tr\mathrm{e}^{(-2\mathrm{i}k_1 L)}\mathrm{e}^g) = 0. \tag{17}$$

Here k_1 should be the propagating wavenumber. Written in a matrix form Eq. (17) becomes

$$\begin{bmatrix} a_{11} & a_{12} \\ a_{21} & a_{22} \end{bmatrix} \begin{bmatrix} v_{n^+} \\ v_{n^-} \end{bmatrix} = \begin{bmatrix} 0 \\ 0 \end{bmatrix}. \tag{18}$$

The zeros of the determinant of the coefficient matrix in the above equation give the propagation constant g.

2.1.3. Discussion

In this subsection, the propagation constant computed for the three-layered beam using the formulation of the previous section is presented. Also, its dominant features are explained by comparison with two elementary models. These two elementary models are based on the Euler theory and the Timoshenko theory respectively. In these two models, the properties (Young's Modulus and area moment of inertia) are averaged over the cross-sectional area in order to arrive at a homogenous equivalent damped model of the three-layered beam. The derivation of the equivalent models being elementary, it is not presented here.

Fig. 4 shows the propagation constants for the Euler equivalent, the Timoshenko equivalent and the three-layered analytical theory. The Euler equivalent beam behaves like the homogeneous Euler beam (as shown in Fig. 1) and differs significantly from the three-layered beam. The three-layered beam model is kinematically closer to Timoshenko theory. However, the Timoshenko equivalent model approximates the three-layered theory more accurately in the attenuation zones. Whereas, in the propagation zones the Timoshenko equivalent model is closer to Euler equivalent theory (which is very close to Euler theory). Thus, Timoshenko equivalent theory gives us a special insight into the propagation constant.

In equivalent theories, because of the averaging process across the cross-section, the damping is negligible (since only the visco-elastic layer is modelled with damping). The three-layered beam having no such averaging does have significant damping. Despite this difference, the peaks in the attenuation zones for the Timoshenko equivalent and three-layered theories are close to each other. So damping plays a negligible role in the attenuation zone peaks. This zone is characterized by the transmission coefficient across a simple support (to be discussed later). In contrast, the propagation zone behaviour is strongly dependent on damping. Thus, in the layered theory, the propagation zone troughs exhibit significant attenuation unlike the Timoshenko theory in which damping is negligible.

The role of damping at the troughs of the propagation constant curve needs to be demonstrated, which is done in the next section using a damped homogenous infinite periodic Euler beam.

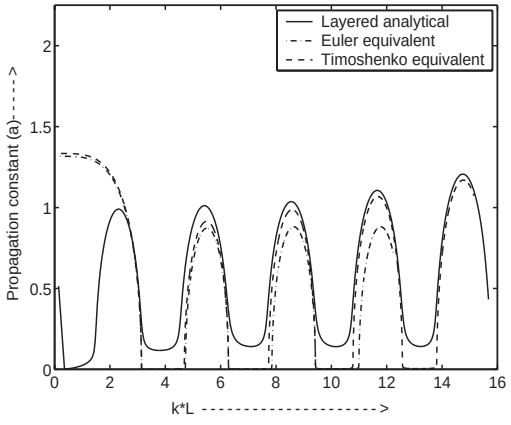

Fig. 4. Variation of propagation constant '*a*' for the layered analytical, Euler equivalent and Timoshenko equivalent theories as function of non-dimensional frequency *kL*.

2.1.4. Simplified formula for the propagation constant

The formula for propagation constant for a periodic homogeneous beam in the case of Euler theory can be given as [2]

$$\cosh(g) = \frac{\cos(kL)\sinh(kL) - \sin(kL)\cosh(kL)}{\sinh(kL) - \sin(kL)}. \tag{19}$$

The $\cosh(kL)$ and $\sinh(kL)$ values are almost same if the value of kL is more than π. And at higher kL values the hyperbolic sine and cosine values are much larger than sine and cosine values. So the above equation can be simplified (for large values of kL) as

$$\cosh(g) = \cos(kL) - \sin(kL). \tag{20}$$

In the above equation imaginary part of $\cosh(g)$ is zero. If we consider damping in the form of complex elastic modulus $E(1 + i\eta)$ (η being half of the damping coefficient), then the wavenumber becomes complex, of the form $k(1 - i\eta/4)$) (see Appendix D for details). Let us denote the wavenumber as $k_1(1 - i\eta_l)$. So if damping is considered, the above Eq. (20) becomes

$$\begin{aligned}\cosh(g) &= \cosh(k_1 L\eta_l)(\cos(k_1 L) - \sin(k_1 L)) \\ &\quad - i\sinh(k_1 L\eta_l)(\cos(k_1 L) + \sin(k_1 L)) \\ &= \mathrm{Re}(\cosh g) + i\,\mathrm{Im}(\cosh g).\end{aligned} \tag{21}$$

Eq. (21) simplifies to Eq. (20) upon substituting $\eta = 0$.

2.1.5. Discussion

Fig. 5a shows that whenever $|\cosh(g)|$ value is above 1, stop bands occur and when the value is between -1 and 1, pass bands occur. The simplified formulas for propagation constant (Eqs. (20) and (21)) give accurate results when the value of kL is above 0.75π.

Fig. 5b shows the propagation constant 'a' for the undamped and damped cases. The damped curve rises with kL, attenuating the propagation zones as well. In the same figure are plotted the $\mathrm{Re}(\cosh g)$ curves for the undamped and the damped case. While the undamped curve oscillates with a uniform amplitude, the damped case oscillates with increasing amplitudes. The peaks of the oscillations coincide with the peak locations of the attenuation zones of the damped propagation constant curve. Thus, damping influences the peaks of the attenuation zones. It should be noted

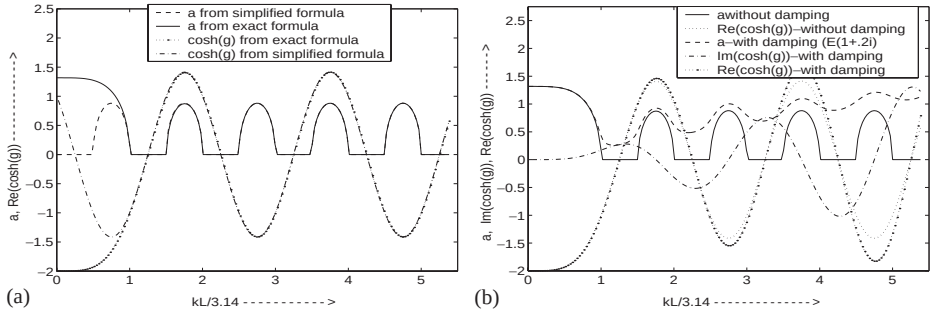

Fig. 5. (a) Propagation constant 'a', $\cosh(g)$ without damping. (b) Propagation constant 'a', $\mathrm{Re}(\cosh(g))$, $\mathrm{Im}(\cosh(g))$ with damping for Euler theory as function of non-dimensional frequency in a periodic homogeneous beam.

that the Re(cosh g) starts to differ from the undamped curve only when $k_1\eta L$ exceeds the value 1. Thus, we call this is a weak dependence on damping.

Also, plotted is the Im(cosh g) which has its peaks at the centers of the propagation zones. The Im(cosh g) is zero for the no damping case (Eq. (20)). It has its maximum value at the centre of the pass bands (i.e., at $n\pi + \pi/4$, $n = 1, 2, 3$). The maximum value of the imaginary part in Eq. (21) will occur at $n\pi + \pi/4$ ($n = 1, 2, 3, \ldots$), since $(\cos(k_1 L) + \sin(k_1 L)$ value is maximum when $k_1 L = n\pi + \pi/4$ ($n = 0, 1, 2, \ldots$). From Fig. 6, one can observe that the maximum value of $\cosh^{-1}(\mathrm{Im}(\cosh g))$ is touching the minimum values of the propagation constant in the pass band. It can be seen that at the troughs of the damped 'a' curve, the $\cosh^{-1}(\mathrm{Im}(\cosh g))$ is the sole contributor. This imaginary part strongly depends on damping, since it is zero for no damping. Here, the $\cosh^{-1}(\mathrm{Re}(\cosh g))$ is zero. And similarly, where the real part is a contributor, i.e., at the peaks, the imaginary value is zero. Thus, the amplification at the peaks is due to the real part and at the troughs due to the imaginary part.

There is another factor which influences the peak attenuations in addition to damping. This is the transmission loss of a flexural wave incident on a simple support in an infinite beam. This factor is constant for Euler theory and depends on frequency for Timoshenko theory. This factor dominates over damping at the peaks of the attenuation zones. This issue is discussed in the next section.

2.1.6. *Transmission and reflection coefficients for a simply supported infinite beam*

In this section, the transmission and reflection coefficients are derived for a flexural wave incident on a single support in an infinite beam. Timoshenko Beam Theory [1,30,31] is used and later specialized for Euler theory at low frequencies. In Timoshenko theory, there occur two wavenumbers k_1 and k_2. The k_2 wavenumber decays faster and hence the incident wave depends only on k_1. Considering an incident wave in section 1 (see Fig. 7) and using support conditions for the two reflected and two transmitted waves, one can obtain the transmission and reflection coefficients for the propagating waves as

$$r = \frac{(k_2^2 + k_s^2)\mathrm{i}k_1}{(-k_1^2 + k_s^2)k_2 - (k_2^2 + k_s^2)\mathrm{i}k_1} \quad \text{and} \quad t = \frac{(-k_1^2 + k_s^2)k_2}{(-k_1^2 + k_s^2)k_2 - (k_2^2 + k_s^2)\mathrm{i}k_1},$$

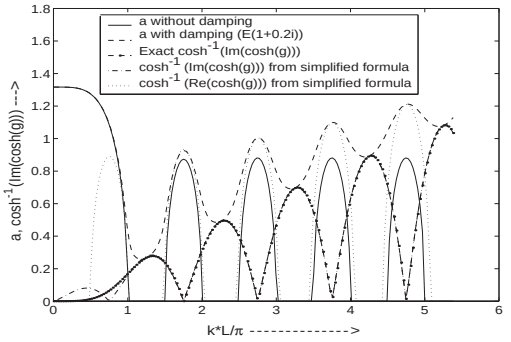

Fig. 6. Variation of propagation constant 'a' and $\mathrm{Re}(\cosh^{-1}(\mathrm{Im}(\cosh(g))))$ with/without damping for Euler theory as function of non-dimensional frequency in a periodic homogeneous beam.

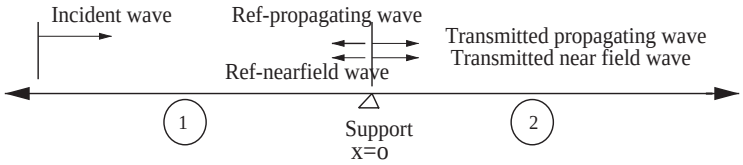

Fig. 7. Sketch of an infinite beam with a single simple support.

where k_s is the shear wavenumber [31]. As k_s is proportional to the frequency, at lower frequencies its value is very less and can be neglected. So the transmission coefficient becomes

$$t = \frac{-k_1^2 k_2}{-k_1^2 k_2 - \mathrm{i}k_2^2 k_1}. \tag{22}$$

And at lower frequencies, k_1, k_2 are equal, and Euler theory is approached. Hence, the above equation can be written as

$$t = \frac{\mathrm{i}k}{\mathrm{i}k - k} = \frac{\mathrm{i}}{\mathrm{i} - 1} = 0.5 - 0.5\mathrm{i}. \tag{23}$$

One can obtain the same result by directly using the Euler Beam Theory. Thus, at low frequencies both theories give the same values for the coefficients. The coefficients are independent of frequency and other physical properties of the beam. This is not true for Timoshenko theory as we have seen above.

So far we have seen how imaginary part of $\cosh(g)$ influences the troughs of the 'a' curve and how the real part influences the peaks for high damping. For moderate and low damping it will be seen that the peaks of the curve are more dependent on the transmission coefficient. In order to prove this we need to know the relation between the transmission coefficient 't' and $\cosh(g)$. The transmission coefficient and $\cosh(g)$ are related through [2]

$$\cosh(g) = \mathrm{Re}\left(\frac{1}{t}\mathrm{e}^{\mathrm{j}kL}\right), \tag{24}$$

where L is the span length in the periodic beam. The above equation is for the undamped case. For the damped case, the equation is

$$\cosh(g) = \frac{1}{2}\left(\frac{1}{t}\mathrm{e}^{\mathrm{j}kL}\mathrm{e}^{k\eta_l L} + \frac{1}{t^*}\mathrm{e}^{-\mathrm{j}kL}\mathrm{e}^{-k\eta_l L}\right). \tag{25}$$

Now, for Euler Beam Theory the transmission coefficient remains the same regardless of whether there is damping or not. This can be easily seen in Eq. (23) by taking k to be complex (which is the effect of damping). And since, $1/|t|$ forms the envelope of the $\cosh(g)$ curve, the peaks remain unaffected. Thus, the troughs are raised while the peaks remain constant for the damped 'a' curve using Euler theory (as seen in Fig. 8a).

In case of Timoshenko Beam Theory, the expressions for t are not so clean and hence are plotted in Fig. 8b as a function of kL. It can be seen that t shows negligible change upon introduction of damping. However, it does change with frequency. Thus, envelope behavior of the 'a' curve follows that of $1/|t|$ as expected. In Fig. 8b, the $1/|t| + c$ curve is superposed on the propagation constant curve. The curve is almost tangential to the peaks of 'a'.

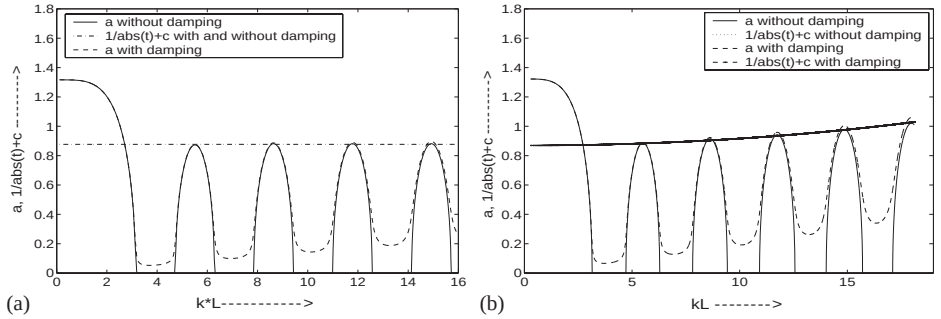

Fig. 8. Propagation constant 'a', and transmission coefficient 't' for (a) Euler theory, (b) Timoshenko theory as a function of non-dimensional frequency kL in periodic homogeneous beams.

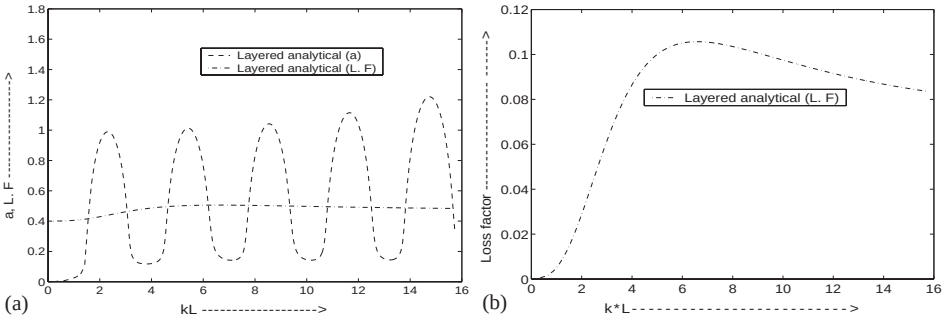

Fig. 9. (a) Propagation constant 'a' for and loss factor (L.F) for layered theory. (b) Loss factor as a function of non-dimensional frequency kL in periodic layered beam.

The entire above discussion holds good for the three-layered periodic beam model, which is the primary goal of this study. It should be mentioned in this context that the loss factor for three-layered sandwich beams have been computed by researchers [2,16,24,26] and it shows a typical increase and then a decrease with respect to kL. Since the loss factor is a function of damping, the troughs of the propagation constant curve of the three-layered periodic beam model does follow this trend as shown in Fig. 9. The peak however, is still a function of the transmission coefficient and does not show the loss factor trend.

3. Part II: finite element analysis

3.1. Introduction

As was mentioned in the introduction at the beginning of the paper, the second part deals with FEM modelling of the three-layered periodic beam (Fig. 10). A numerical approach is needed in order to model the damping layer as inserts (see Fig. 11). Here, initially the FEM model of the continuous layered beam is developed and compared with the previous analytical results. The differences are approximately accounted for before proceeding to the modelling of inserts (refer to the main introduction section at the beginning of the paper).

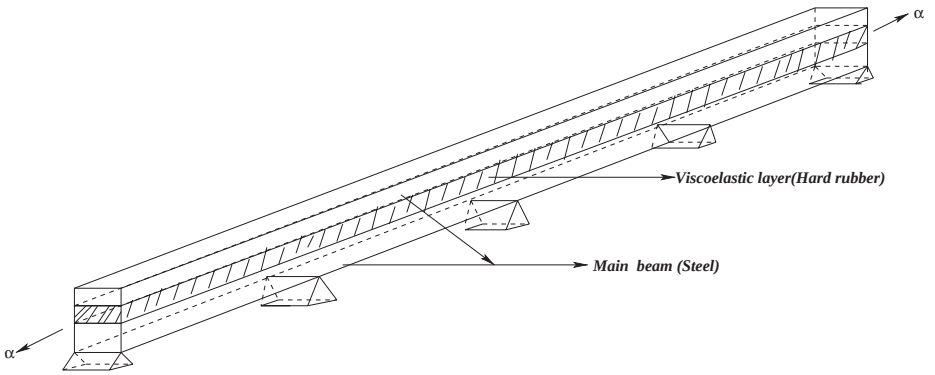

Fig. 10. A schematic of a three-layered periodically supported beam.

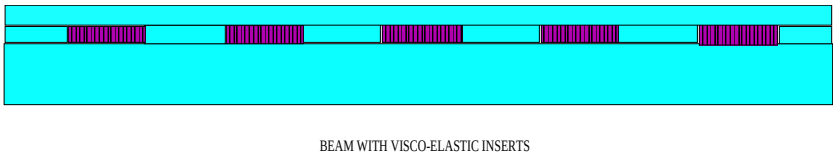

Fig. 11. A schematic of one span in an infinite periodic beam with visco-elastic inserts.

In the following subsection (Section 3.2), the specifics of the two ANSYS elements capable of modelling beams are discussed and the actual configuration used in this study (number of layers, etc.) is presented. Then, in Section 3.3 the method to compute the propagation constant is detailed. In Section 3.4, the various cases in FEM are listed the results of which are compared with the analytical method. In Section 3.5, the comparison between FEM and homogenous periodic beam theories and the analytical three-layered periodic beam model is discussed. Also, the non-rigorous internal consistency within FEM is validated. After the comparison, FEM studies are presented for various layer configurations (thickness, location, etc.) in Section 3.6. Section 3.7, presents the propagation constants for the beam with visco-elastic inserts. The conclusions are presented in Section 4.

3.2. Specifics of the B2D and S73 models

B2D is a 1-D Euler beam element which has two degrees of freedom (one vertical translation and one rotation) at each node. In the model when a single homogenous span is modelled using B2D, a single layer is considered. For three-layered Euler cases, each material layer is again modelled using a single layer of B2D element. S73 element is a 3-D element with six degrees of freedom at each node. With S73 also, each material layer (whether homogenous or three-layered) is modelled using a single layer in the thickness direction.

3.3. Steps to find coefficient matrix using FEM model

Similar to the infinite homogeneous periodic beams [2] where the propagation constants were derived analytically, here also a single span of a beam is considered with boundary conditions $v_y(0) = 0$, $v_y(L) = 0$ at the ends. As shown in Fig. 12, a moment (M_z) is applied at support 1 at all

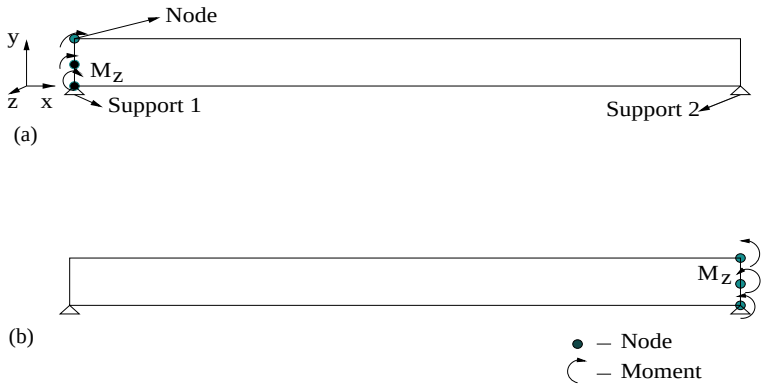

Fig. 12. A schematic of FEM model: (a) to find α_{11}, α_{12} by applying moment M_z at support 1; (b) to find α_{22} by applying moment M_z at support 2.

the nodes in the vertical plane, and the minimum rotations computed at supports 1 and 2 in the same horizontal plane. Using the total moment and the rotations, the moment impedances α_{11}, α_{12} are obtained. Similarly, by applying a moment at support 2 one can find the moment impedances α_{22}, α_{21}. The expression for $\cosh g$ is then given by [2]

$$\cosh g = \frac{(\alpha_{11} + \alpha_{22})}{2\alpha_{12}},$$

where, in general, α_{11} and α_{22} are different except when the central layer is symmetric in which case they are equal. The values of α_{12} and α_{21} are however always equal.

3.4. FEM model cases

In this section, we list out the specific cases studied in FEM using the two elements B2D and S73, for validation against analytical models. The cases are as follows:

1. The *homogeneous* Euler beam is modelled using B2D element. The results for a periodic beam are compared with the results from the analytical approach. (Section 3.5.1)
2. The *homogeneous* beam is modelled using S73 element and is done in two ways (Section 3.5.1):
   a. All the three shear strains ($\gamma_{xy}, \gamma_{yz}, \gamma_{xz}$) are suppressed.
   b. Only transverse shear strain (γ_{xy}) is allowed.
   c. Both the above methods are compared with analytical results.
3. The *three-layered* beam is modelled and is done in three separate ways (Section 3.5.2):
   a. The transverse shear (γ_{xy}) is allowed in the visco-elastic layer but all the three shear strains are suppressed in the parent material.
   b. All the three shear strains ($\gamma_{xy}, \gamma_{yz}, \gamma_{xz}$) are allowed in the visco-elastic layer. No shear strains are allowed in the parent material.
   c. All the three shear strains ($\gamma_{xy}, \gamma_{yz}, \gamma_{xz}$) are allowed in the visco-elastic layer. And only transverse shear (γ_{xy}) is allowed in parent material.
   d. The above three results are compared with the three-layered analytical model.

It is important to note that the S73 element co-ordinate system should be taken for giving orthotropic properties (see ANSYS Elements manual for details).

In this investigation, the following materials and properties have been assumed. Parent material for the beam is steel and the visco-elastic material is hard rubber. The Young's modulus, density and the Poisson ratio of steel are $E = 20.71e^{10}$ N/m^2, $\varrho = 7850$ kg/m^3, $v = 0.25$, whereas for the hard rubber the values are $E = 20.71e^{8}$ $(1 + 0.5i)$ N/m^2, $\varrho = 3850$ kg/m^3, $v = 0.4$ respectively. For all layered beam cases the total thickness and breadth of the beam is 10 cm. The length of the each span in a periodic beam is 1 m, if it is not mentioned in the corresponding sections. For all the homogeneous beam cases the thickness and breadth of the beam is 5 cm. In most examples presented in this paper, within the height of 10 cm, the visco-elastic material is placed 2 cm below the top surface. And unless mentioned the visco-elastic layer is 2 cm thick. This leaves 6 cm parent material below the visco-elastic layer. This is called the 2-2-6 configuration.

3.5. Discussion

3.5.1. Euler and Timoshenko beam theories vs. FEM (Homogenous periodic beam)

We begin the FEM 'validation' by comparing the FEM models with the simple and established Euler and Timoshenko analytical theories for homogenous periodic beams. The FEM model is done in ANSYS using the B2D element and the S73 element which can optionally incorporate the transverse shear strain.

Fig. 13 shows the propagation constants for the periodic homogenous beam using the FEM analysis, the Euler and Timoshenko analytical theories. It can be seen that the B2D element suits the Euler beam theory quite well. The reason being that this element was derived based on Euler beam theory.

In addition to the B2D element, the S73 element was also used by suppressing all shear strains. This was done just to gain confidence in that particular element and see how it compared with B2D element. The curves due to S73 are a little to the right of B2D suggesting higher natural frequencies. The reason for this is that, Euler theory does not allow for normal stresses in the two

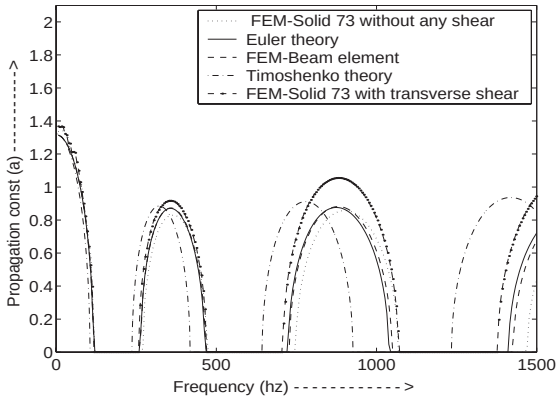

Fig. 13. Variation of the propagation constant from FEM and analytical theories as a function of frequency in a periodic homogeneous beam.

transverse directions, whereas S73 element is a 3-D element with six degrees of freedom at each node. Even though we set displacements free at the boundaries, the normal stresses within the cross-section are not zero. This makes the beam stiffer and raises the natural frequencies. As evidence of this, the cross-section was reduced, after which S73 results approached those of Euler theory. If transverse shear is allowed for S73 element then the curve shifts a little towards the left.

In Appendix E the dispersion expression and the curve for Timoshenko theory are given. Timoshenko theory being a refinement over Euler theory, three additional terms appear which are not present in Euler theory. They are the last three terms in Eq. (E.1). And they denote, respectively, the effects of rotary inertia, the transverse shear and a coupling term between the two. Fig. 23 shows a plot of the wavenumber as a function of the frequency (the dispersion curve). The effects of each of the terms mentioned earlier can be seen in the dispersion curve. Each term raises the wavenumber curve over and above that of the Euler curve. Yet, the maximum effect is that of the coupling term. Looking at the total Timoshenko dispersion curve, a given value of the wavenumber k occurs at a frequency lower than that for Euler theory. Thus, the same wavelength occurs at a lower frequency which implies that resonances are lower for Timoshenko theory and the influences are in proportion to the effects of the three terms on the dispersion curve. It can be seen that the Timoshenko theory differs from Euler and the two FEM models even at low frequencies. The shift of the curve is due to rotary inertia and shear factor. The increase in attenuation is due to the frequency dependency of transmission coefficient (t) [2], which in turn depends on both shear and rotary inertia.

The last case studied is S73 with transverse shear strain allowed. In this case the magnitude of attenuation in the attenuation zones is more compared to the Timoshenko beam theory. Even though Timoshenko theory is a higher order theory in comparison to Euler theory, it is not consistent with 3-D elasticity and hence differences are expected in comparison with S73 element. Yet, the exact reason for the shift between analytical Timoshenko theory curve and this model curve is not clear. This model lines up closely with Euler theory which has no shear deformation. The stiffness due to the two transverse normal shear stresses seems to be compensated by the additional compliance given by the transverse shear deformation. When the curves are plotted on a kL basis the peaks for all the cases line up.

3.5.2. Three-layered analytical method vs. FEM (continuous visco-elastic layer)

In this section, the three-layered analytical model proposed earlier is compared with FEM analysis from ANSYS in which the S73 element is used. Since the Solid 73 element is capable of modelling all the three shear strains, three separate cases are studied, one where all the three shear strains ($\gamma_{xy}, \gamma_{yz}, \gamma_{xz}$) are set to zero in the parent material and only transverse shear (γ_{xy}) is allowed in the visco-elastic layer (FEM1). And case two where again all the three shear strains ($\gamma_{xy}, \gamma_{yz}, \gamma_{xz}$) are set to zero in the parent material and all the shear strains are allowed in the visco-elastic material (FEM2). And case three where the transverse shear strain γ_{xy} is allowed in the parent material, and all shear strains are allowed in the visco-elastic material (FEM3).

Fig. 14 shows the amplitude of the propagation constants for the analytical method, FEM1, FEM2 and FEM3 cases. The initial high value of the propagation constants in all FEM cases is due to near field waves which are not accounted for in the analytical model. It can be seen that each propagation zone contains a natural frequency of a single span of the infinite beam. The curve has been plotted with the x-axis as frequency and the presence of the three terms mentioned

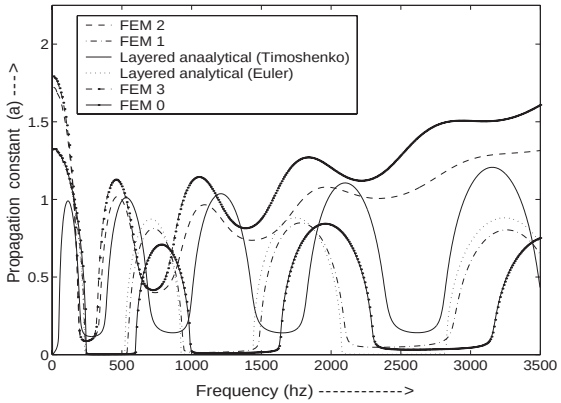

Fig. 14. Variation of the propagation constant for layered analytical (Euler), layered analytical (Timoshenko), FEM1, FEM2 and FEM3 theories as a function of frequency in a periodic layered beam (2-2-6 configuration).

earlier in the analytical layered model drops the natural frequencies, so that within the same frequency range, the number of natural frequencies and the peaks are more compared to the FEM1. Here too, the three-layered Euler beam aligns itself with FEM1, the reason for which was given in the last part of the previous section. The S73 element for a homogenous beam with zero shear strain and only (γ_{xy}) lie on either side of the Euler analytical beam theory (see Fig. 13). Next, for a three-layered beam, the S73 element again with zero shear strains (FEM0) leads the Euler curve and FEM1 aligns itself with Euler theory (see Fig. 14). The reasons have been seen in the previous section. From this the performance of FEM S73 element is considered satisfactory for further parametric studies.

It is however not guaranteed that FEM1 or FEM2 will converge onto FEM3, i.e., if restrictions on shear strains are removed in FEM1 or FEM2 in small increments do we arrive at FEM3? If a new phenomenon appears somewhere along the way, the convergence will not occur. To see this, we introduce small changes in the number and magnitude of shear strains within the parent and the visco-elastic material till we reach the FEM3 model (no constraint on shear strains in visco-elastic material), thus ensuring a continuous sequence of changes in the results. A drastic change in the propagation constant value for a small change in the restraint of shear strains would imply some form of singularity or a radically different phenomenon. The validity of FEM3 is established through this mechanism of consistency.

Thus, we begin by introducing transverse shear strains only in the visco-elastic material. This is shown as FEM1 in Fig. 14 and its amplitudes in the propagation zone are slightly higher than the layered Euler case (this is due to damping as discussed above). After this, each shear strain ($\gamma_{xy}, \gamma_{yz}, \gamma_{xz}$) is taken from total restraint to no restraint in small steps for the visco-elastic layer. The FEM2 is the result of releasing all shear strains from restraint. From the earlier argument this establishes the validity of FEM2. An additional point in favour of FEM2 is that the number of peaks within a given frequency match with that of three-layered analytical model. The attenuation in FEM2 is definitely more due to energy dissipated in all the shear strains predominantly due to in-plane shear strain (γ_{yx}).

In order to model thicker beams, transverse shear strain should be allowed in the parent material. Once FEM2 validity is justified, for the same model the transverse shear strain (γ_{xy}) is allowed in the parent material, which is the case FEM3. Looking at Fig. 14, the attenuation increases for this model due to the presence of a dissipative mechanism in the parent material as well. The attenuation peaks shift towards the left which implies an increase in the number of natural frequencies for FEM3. The increase in the attenuation (in FEM3) is not much but significant, when compared with FEM2.

In this approximate manner, we find FEM results reliable for further parametric studies. It should be mentioned here, that most of the visco-elastic materials have low elastic moduli. So one-dimensional theories will not give accurate results. It is better to model these materials with 3-D elements and the parent material to be modelled with 1-D elements.

3.6. Wave attenuation in a periodic layered beam

3.6.1. Variation of the propagation constant with the position, length and thickness of the visco-elastic layer

In the above two subsections, the 'validity' of the FEM2 and FEM3 models using S73 of ANSYS has been established. It was shown that the FEM3 model gives more attenuation than FEM2. But the variation in the results is not much compared to the FEM2. However, for understanding and modelling, the FEM2 model is simpler than the FEM3 model. Hence from this section onwards most of the case studies will be done using FEM2 and a few results using FEM3 will also be presented.

The first case study involves the influence of the y locations (see Figs. 2 and 15) of the visco-elastic layer on the propagation constant. For this purpose a 2 cm thick visco-elastic layer is taken with a total beam thickness of 10 cm, i.e., the parent material of the beam is 8 cm thick. The visco-elastic layer is placed at various y locations within the beam and the propagation constants computed. Fig. 15 shows the propagation constants for four locations of the visco-elastic layer, 2 cm from the top, 1 cm from the top, middle of the beam and top of the beam (top surface free) using two FEM models (FEM2 and FEM3). The propagation constants are maximum when the

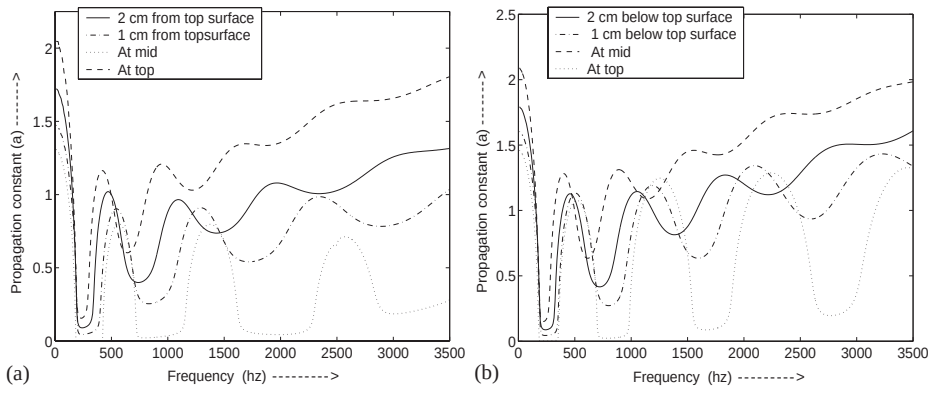

Fig. 15. Variation of propagation constant for (a) FEM2 model and (b) FEM3 model for various positions of the visco-elastic layer measured from top surface of the beam as function of frequency in a periodic layered beam.

layer is at the centre and least when it is at the top. This is because the shear strain is maximum when the visco-elastic layer is at the centre and it behaves like a constrained layer. It can also be seen that for a given maximum frequency of interest the number of peaks are more when the elastic layer is at the middle. This in turn implies that there are more number of natural frequencies and that the structure is weaker as result. This weakening effect can be seen as the progressive left shifting of the peaks as the layer is placed more towards the centre.

The second study is with respect to the length of the span (Fig. 16a). The visco-elastic layer is placed at the centre with respect to the thickness of the beam. The propagation constants for the various lengths of the spans are plotted. With increase in length the natural frequency drops and hence the peaks shift to the left. Also the attenuation at a given frequency is higher for a longer length. This is due to the decay of the wave across the longer length.

The third study is with respect to the thickness of the visco-elastic layer. Fig. 16b illustrates how attenuation increases with the thickness of the visco-elastic layer. The energy dissipated within the visco-elastic layer is proportional to its thickness (one needs to integrate over the thickness to obtain the strain energy). Hence, increasing the thickness increases the attenuation. In the figure, the case with 3 cm thickness placed 2 cm below the top layer is almost the same as that with 2 cm thickness placed 2 cm below the top layer. However, with a 3 cm layer thickness, the structure is weaker as indicated by the left shift of the peaks implying an increase in the number of resonances. When the 3 cm layer is 1 cm below the top layer, its performance is lower than the 2 cm layer which is 2 cm below the top layer. This of course is due to the fact that a central layer gives more attenuation. One could thus choose a best possible thickness and location with attenuation and strength in view (Fig. 17).

The three factors influencing the propagation constant are the thickness, the location of the visco-elastic layer and the length of the span. Amongst the three, the position is the dominant factor affecting the propagation constant. We have found an equation which non-dimensionalizes the propagation constants and aligns them approximately along a single curve. The propagation constant calculation is intensive since zeros of a fourth order polynomial have to be found numerically for every configuration. Using this equation (Eq. (26)) one can obtain the new

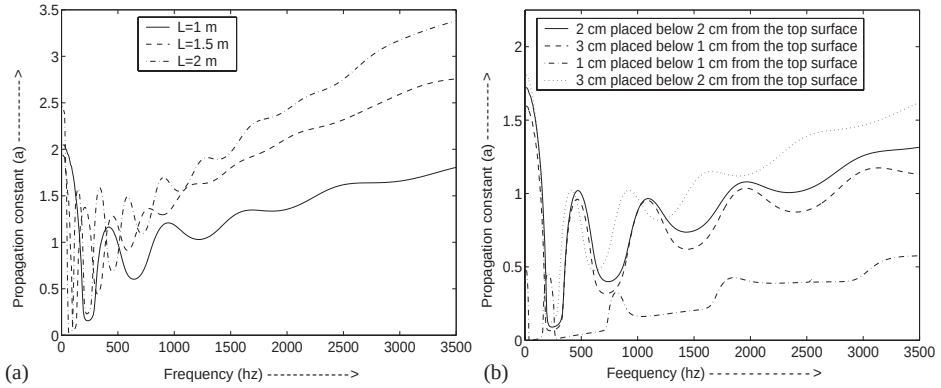

Fig. 16. Variation of the propagation constant for (a) different span lengths with visco-elastic layer at the centre of the beam thickness and (b) different thicknesses of the visco-elastic layers at different positions from the top surface as a function of frequency kL (results using FEM2 model).

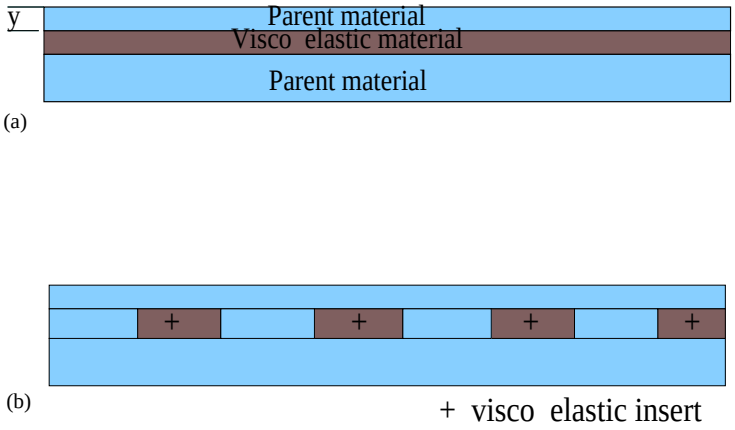

Fig. 17. (a) Three-layered beam with a continuous visco-elastic layer. (b) Beam with visco-elastic inserts.

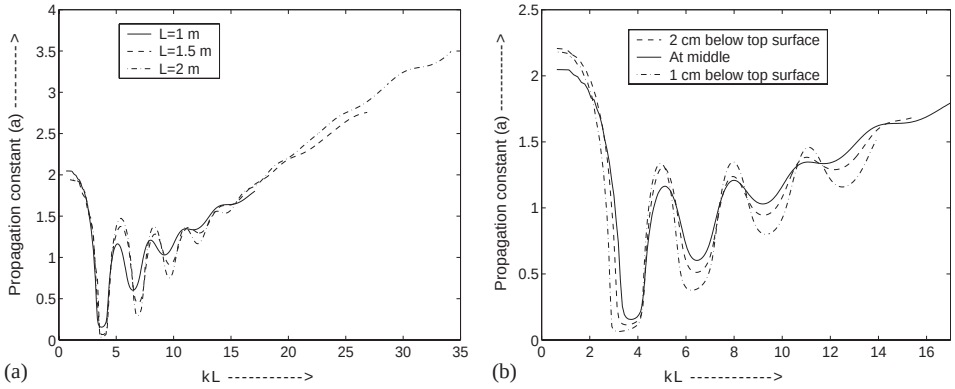

Fig. 18. Variation of the non-dimensionalized propagation constants for (a) different lengths of the visco-elastic layer centred with respect to the beam thickness and (b) different y locations within the thickness, as a function of non-dimensional frequency kL after applying the formulae (26) (results using FEM2 model).

propagation constant pc_n for a new thickness, location and span length based on the propagation constant for a central layer (pc_{mid}) and original length (L). k_{mid} is the wavenumber in the central position and k_n is the new wavenumber. y_n is the new neutral axis position from the central axis and L_n is the new length. d is the central axis position from the bottom or top most fibre.

$$pc_n = pc_{mid}\,\frac{(k_n L_n)}{(k_{mid} L)}\left(\frac{d - y_n}{d}\right)^4. \tag{26}$$

Figs. 18 and 19 show the non-dimensional propagation constants for FEM2 and FEM3 respectively. Fig. 18a is for various lengths while the visco-elastic layer is centred and Fig. 18b for various y locations of the visco-elastic layer. These figures are obtained by using Eq. (26). As mentioned earlier, with increase in length of the span, the natural frequency drops and attenuation at a given frequency is higher for a longer length. This is due to the decay of the wave

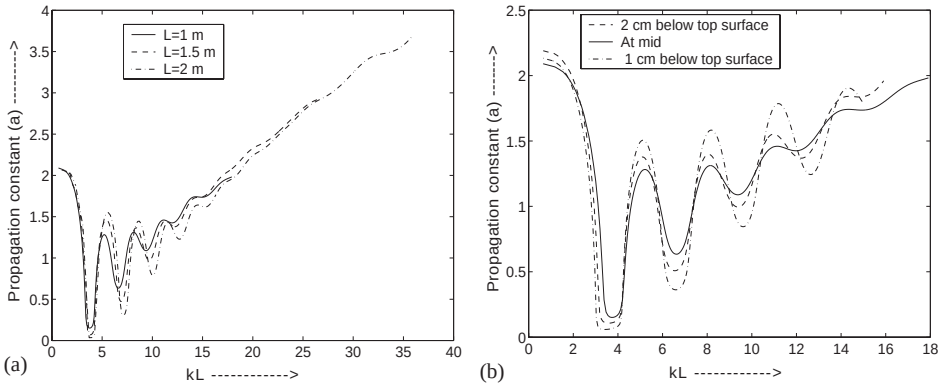

Fig. 19. Variation of the non-dimensionalized propagation constants for (a) different lengths of the visco-elastic layer centred with respect to the beam thickness and (b) different y locations within the thickness, as a function of non-dimensional frequency kL after applying the formulae (26) (results using FEM3 model).

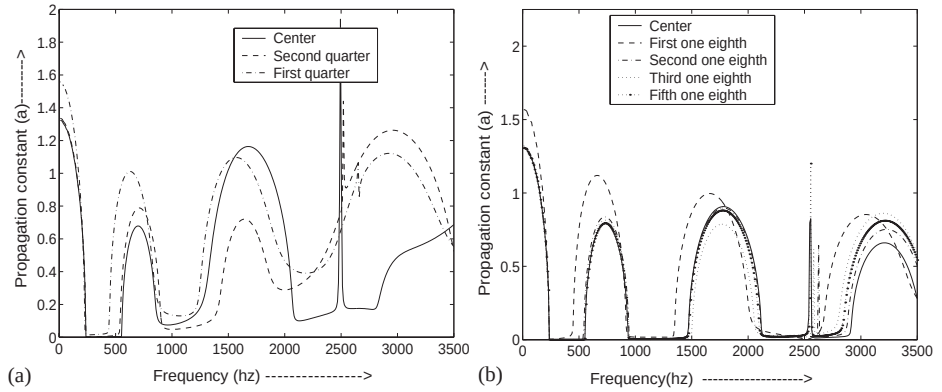

Fig. 20. Variation of the propagation constant in layered beam with visco-elastic insert of (a) length $0.25L$ at different positions along the span, (b) length $0.125L$ at different positions along the length of the span as a function of frequency (2-2-6 configuration).

across the longer length. Fig. 19 shows the exact same cases but for FEM3. Thus, the same Eq. (26) holds good.

3.7. Wave attenuation in a periodic beam with visco-elastic inserts

3.7.1. Studies with quarter and one-eighth span length inserts

In all layered beam cases presented so far, the visco-elastic layer is continuous throughout the span of the beam. In the following cases, the visco-elastic layer is placed in the parent beam material in the form of inserts (as shown in Fig. 17b) instead of a continuous layer. Different cases are studied with different length, number and location of the inserts. In Fig. 20 a single insert of length equal to a fourth of the span is placed at different locations along the span and its influence on the propagation constant presented. It is seen that the location has very little influence on the

first attenuation band. Since each attenuation band is related to a particular flexural mode of the span [2,3], the location of the insert between the antinodal regions for that mode produces a high attenuation in that band. For example, when the insert is placed at the center of the span, it lies entirely between the two nodes of the third mode and hence the third attenuation zone is amplified. Similarly, for the fourth mode since the antinodal region is exactly equal to the length of the insert, any location which covers the antinodal region amplifies the fourth attenuation zone. It is for this same reason that any location has almost the same influence on the first attenuation zone.

From the figure we can observe that for the central position we get a sharp peak just before the fourth attenuation band. The reasons for this are yet unclear. It is of course true that since the propagation constant is derived from the ratio of the rotations at the two ends of the beam, the denominator rotation is going to zero. This is indicative of a complex mode shape (as seen in the finite beams cases [3]) which cannot happen in case of infinite beams. An important fact to be noted is that, the longitudinal, torsional and in-plane flexural natural frequencies all occur at that frequency. However, the beam is excited anti-symmetrically with respect to all these modes and hence there is no way of exciting them. It could also be a numerical issue.

Fig. 20(b) shows the case for an insert one-eighth the span length. Here also, several locations are chosen. The behaviour is similar to that of the one-fourth case. The attenuation levels in the propagation zone are much lower than the three-layered continuous case. It is to be expected since there is not much material to absorb the vibration.

3.7.2. Different lengths of visco-elastic material inserted at center of the beam span

Fig. 21 illustrates the variation of the propagation constant for various lengths of visco-elastic inserts placed at center of the periodic span. As the length of visco-elastic layer decreases, the attenuation decreases throughout the frequency range. The case with an insert equal to one-eighth span almost behaves like a homogeneous beam. The one-half case seems to work well in comparison with the continuous visco-elastic layer. The left shift of the peaks is lesser than the continuous layer which implies a lesser number of natural frequencies within the same frequency range and hence a stronger construction.

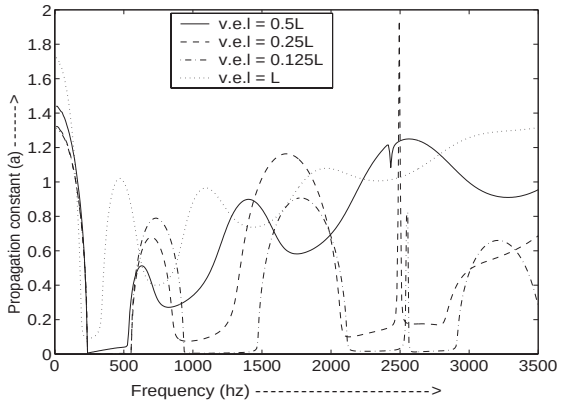

Fig. 21. Variation of the propagation constant for visco-elastic insert lengths L, $0.5L$, $0.25L$ and $0.125L$ located at center of the span as a function of frequency (2-2-6 configuration).

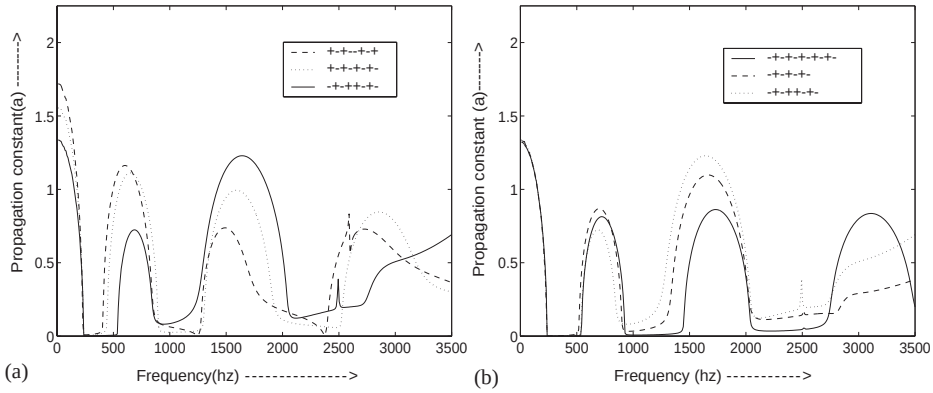

Fig. 22. Variation of the propagation constant in layered beam with visco-elastic inserts: (a) 4 inserts of length $0.125L$ placed at a time within a span at different positions; (b) inserts of different lengths, but of total length equal to $0.5L$, + indicates position of insert in the total span (2-2-6 configuration).

3.7.3. *Multiple visco-elastic inserts of total length equal to half the span*

In this section, propagation constants are found for cases with multiple inserts, the sum of whose length is equal to half the span. In these figures '+' indicates the presence of the visco-elastic insert, and '−' represents the main beam material at the same 'y' position.

In Fig. 22a four inserts are placed at the centre of the parent material each of length equal to one-eighth the span. From the figure we can say that the third case is working well. If we compare any of these three cases with the results of the previous sub-section, we can say that a single visco-elastic insert of length equal to half the span located at the centre will work better than 4 pieces inserted at different locations. However, from the strength point of view 4 inserts are better.

In Fig. 22b we look at 3, 4 and 5 inserts of lengths one-sixth, one-eighth and one-tenth the span, respectively. From the Fig. 22b we can say that the four $(1/8)L$ inserts will work better than the other two cases. An insert length of $(1/10)L$ is very small, so the shear is small. However, for the three $(1/6)L$ beam length inserts the chance to shear is better than the $(1/8)L$ length inserts, but the position of the inserts is not conducive for maximum attenuation. The arguments have been presented in the previous subsection.

4. Conclusions

In this two-part investigation, a composite infinite periodically supported beam was studied for understanding its vibration attenuation characteristics. Two distinct cases were presented. The first case was a three-layered infinite periodic beam with a central continuous visco-elastic layer. This system was modelled using Timoshenko theory kinematic assumptions and analyzed using wave propagation methods. Equations were derived to compute the propagation constant for this periodic beam. It was shown that the propagation constant curve rises with kL over the undamped curve. Features of the propagation curve were explained in detail using several simple beam theories. The attenuations at the troughs are strongly dependent on the degree of damping while the attenuations at the peaks are more dependent on the transmission coefficient of the

support for low and moderate damping. For high damping, however, the peak attenuations also depend on damping.

The second case involved a periodic beam with visco-elastic inserts. This entire study was based on finite element methods (FEM). Prior to modelling the inserts, the FEM results were validated by comparing against the results from the previous continuous layer case. Several configurations were tried based on the B2D and S73 elements. Through approximate arguments it was established that the FEM results made physical sense and were as expected.

Then several parametric studies were performed in FEM for a three-layered beam with a continuous visco-elastic layer. The location, thickness and the length of the span were varied and their influence on the propagation constant analyzed. It was found that the maximum dissipation is realized when the visco-elastic layer is centred with respect to the total thickness of the beam, and also when the visco-elastic layer itself is thick and the span is long. An equation for non-dimensionalizing the propagation constants was derived, so that by knowing the values for one configuration those for another could be computed with ease.

Finally, studies were performed using FEM for cases where the central visco-elastic layer is not continuous, but is in the form of inserts. It was found that long inserts are better than short ones. However, long inserts weaken the structure. A single insert is better than several whose total length is the same. An insert placed between the two nodes of a given mode gives the best attenuation. Thus, an insert can be tailored to give the best attenuation for a certain frequency band.

Appendix A

$$
\begin{aligned}
\varphi_1'' &= E_e\xi_L'' + (h_1E_e - 0.5E_1d_1^2)\beta_1'' + (0.5E_2d_2^2 + E_3d_2d_3)\beta_2'' + 0.5E_3d_3^2\beta_3'',\\
\ddot{\varphi}_1 &= -0.5m_e\ddot{\xi}_L - (h_1m_e - 0.5\varrho_1d_1^2)\ddot{\beta}_1 - (0.5\varrho_2d_2^2 + \varrho_3d_2d_3)\ddot{\beta}_2 - 0.5\varrho_3d_3^2\ddot{\beta}_3,\\
\varphi_2'' &= G_e\eta'' + G_1d_1\beta_1' + G_2d_2\beta_2' + G_3d_3\beta_3',\\
\ddot{\varphi}_2 &= -m_e\ddot{\eta},\\
\varphi_3'' &= (E_eh_1 - 0.5E_1d_1^2)\xi_L'' + (E_1d_1^3/3 + E_eh_1^2 - E_1d_1^2)\beta_1''\\
&\quad + (0.5E_2h_1d_2^2 + E_3h_1d_2d_3)\beta_2'' + 0.5E_3h_1d_3^2\beta_3'' - G_1d_1\beta_1 + \mathrm{i}kG_1d_1\eta,\\
\ddot{\varphi}_3 &= -(m_eh_1 - 0.5\varrho_1d_1^2)\ddot{\xi}_L - (\varrho_1d_1^3/3 + h_1^2m_e - \varrho_1h_1d_1^2)\ddot{\beta}_1\\
&\quad - (0.5\varrho_2h_1d_2^2 + \varrho_3h_1d_2d_3)\ddot{\beta}_2 - 0.5\varrho_3h_1d_3^2\ddot{\beta}_3,\\
\varphi_4'' &= (0.5E_2d_2^2 - E_3d_2d_3)\xi_L'' + (0.5E_2h_1d_2^2 + E_3h_1d_2d_3)\beta_1''\\
&\quad + (0.5E_2d_2^3/3 + E_3d_2^2d_3)\beta_2'' + 0.5E_3d_2d_3^2\beta_3'' - G_2d_2\beta_2 + \mathrm{i}kG_2d_2\eta,\\
\ddot{\varphi}_4 &= -(0.5\varrho_2d_2^2 - \varrho_3d_2d_3)\ddot{\xi}_L - (0.5\varrho_2h_1d_2^2 - \varrho_3h_1d_2d_3)\ddot{\beta}_1\\
&\quad + (0.5\varrho_2d_2^3/3 - \varrho_3d_2^2d_3)\ddot{\beta}_2 - 0.5\varrho_3d_2d_3^2\ddot{\beta}_3,\\
\varphi_5'' &= 0.5E_3d_3^2\xi_L'' + 0.5E_3h_1d_3^2\beta_1'' + 0.5E_3d_2d_3^2\beta_2'' + (E_3d_3^3/3)\beta_3''\\
&\quad - G_3d_3\beta_3 + \mathrm{i}kG_3d_3\eta,\\
\ddot{\varphi}_5 &= -0.5\varrho_3d_3^2\ddot{\xi}_L - 0.5\varrho_3h_1d_3^2\ddot{\beta}_1 - 0.5\varrho_3d_2d_3^2\ddot{\beta}_2 - \varrho_3d_3^3/3\ddot{\beta}_3.
\end{aligned}
\tag{A.1}
$$

Appendix B

$$
\begin{aligned}
\Omega_{11} &= k^2 E_e - \omega^2 m_e,\\
\Omega_{12} &= 0,\\
\Omega_{13} &= \left(E_e h_1 - \frac{E_1 b d_1^2}{2}\right)k^2 - \left(m_e h_1 \frac{\varrho_1 b d_1^2}{2}\right)\omega^2,\\
\Omega_{14} &= b\left(\left(\frac{E_2 d_2^2}{2} + E_3 d_2 d_3\right)k^2 - \left(\frac{\varrho_2 d_2^2}{2} + \varrho_3 d_2 d_3\right)\omega^2\right),\\
\Omega_{15} &= b\left(\frac{E_3 d_3^2}{2}k^2 - \frac{\varrho_3 d_3^2}{2}\omega^2\right),\\
\Omega_{22} &= -G_e k^2 + \omega^2 m_e,\\
\Omega_{23} &= \mathrm{i}kbG_1 d_1,\\
\Omega_{24} &= \mathrm{i}kbG_2 d_2,\\
\Omega_{25} &= \mathrm{i}kbG_3 d_3,\\
\Omega_{34} &= \Omega_{14} h_1,\\
\Omega_{35} &= \Omega_{15} h_1,\\
\Omega_{33} &= \left[E_e h_1^2 - E_1 b d_1^2\left(h_1 - \frac{d_1}{3}\right)\right]k^2 - \left[m_e h_1^2 - \varrho_1 b d_1^2\left(h_1 - \frac{d_1}{3}\right)\right]\omega^2 + G_1 b d_1,\\
\Omega_{44} &= b\left(\left(\frac{E_2 d_2^3}{3} + E_3 d_2^2 d_3\right)k^2 - \left(\frac{\varrho_2 d_2^3}{3} + \varrho_3 d_2^2 d_3\right)\omega^2 + G_2 d_2\right),\\
\Omega_{55} &= b\left(\frac{E_3 d_3^3}{3}k^2 - \frac{\varrho_3 d_3^3}{3}\omega^2 + G_3 d_3\right),\\
\Omega_{45} &= \Omega_{15} d_2,\\
\Omega_{ij} &= \Omega_{ji},
\end{aligned}
\tag{B.1}
$$

where

$$
\begin{aligned}
E_e &= b(E_1 d_1 + E_2 d_2 + E_3 d_3),\\
m_e &= b(\varrho_1 d_1 + \varrho_2 d_2 + \varrho_3 d_3),\\
G_e &= b(G_1 d_1 + G_2 d_2 + G_3 d_3).
\end{aligned}
\tag{B.2}
$$

Appendix C

$$
F_s = \eta' G_e + b(G_1 d_1 \beta_1 + G_2 d_2 \beta_2 + G_3 d_3 \beta_3); \tag{C.1}
$$

the bending moment in the third layer (from bottom) is given by

$$M_3 = b\left(\beta_3' \frac{E_3 d_3^3}{3}\right) + b\left(\frac{(\xi_L' + h_1\beta_1' + \beta_2')d_2 d_3^2 E_3}{2}\right); \tag{C.2}$$

the bending moment in the second layer is given by

$$M_2 = b\left(\beta_2'\left(\frac{E_2 d_2^3}{3} + E_3 d_2^2 d_3\right) + \frac{\xi_L'(E_2 d_2^2 + 2E_3 d_2 d_3)}{2}\right) + \frac{\beta_1'(E_2 b h_1 d_2^2 + 2E_3 b h_1 d_2 d_3)}{2} + \frac{\beta_3' E_3 b d_2 d_3^2}{2}; \tag{C.3}$$

the bending moment in the first layer is given by

$$M_1 = \beta_1'\left(\frac{E_1 b d_1^3}{3} + h_1^2 E_e - E_1 d_1^2 b h_1\right) + \frac{\xi_L'(E_e h_1 + E_1 b d_1^2)}{2} + \frac{\beta_2'(E_2 h_1 b d_2^2 + 2E_3 b h_1 d_2 d_3)}{2} + \frac{\beta_3' E_3 b h_1 d_3^2}{2}; \tag{C.4}$$

the longitudinal force is given by

$$F_l = E_e \xi_L' + \beta_1'\left(\frac{2h_1 E_e - E_1 d_1^2 b}{2}\right) + \frac{\beta_2'(E_2 b d_2^2 + 2E_3 b d_2 d_3)}{2} + \frac{\beta_3' E_3 b d_3^2}{2}. \tag{C.5}$$

Appendix D. Slope of the loss factor in Euler beam theory

In Euler beam theory the wavenumber (k) can be found from the following equation:

$$k = \omega^{1/2}\left(\frac{\rho A}{EI}\right)^{1/4}. \tag{D.1}$$

If the Young's modulus is complex ($E(1 + \mathrm{i}\eta)$), where η is half of the damping coefficient. Then Eq. (D.1) becomes

$$k = \omega^{1/2}\left(\frac{\rho A}{E(1+\mathrm{i}\eta)I}\right)^{1/4} = \frac{(\omega/h)^{1/2}(\rho/E)^{1/4}(1-\mathrm{i}\eta)^{1/4}}{(1+\eta^2)^{1/4}} = C\omega^{1/2}\left(1 - \frac{1}{4}\mathrm{i}\eta\right), \tag{D.2}$$

where

$$C = \frac{(1/h)^{1/2}(\rho/E)^{1/4}}{(1+\eta^2)^{1/4}}.$$

Imaginary part in Eq. (D.2) gives the loss factor. The slope of the loss factor between two wavenumbers (k_1, k_2 at different frequencies ω_1, ω_2) is given by

$$\mathrm{Tan}\,\theta = \frac{\mathrm{Im}(k_1) - \mathrm{Im}(k_2)}{\mathrm{Re}(k_1) - \mathrm{Re}(k_2)}, \quad \theta = \mathrm{Tan}^{-1}\left(\frac{\eta}{4}\right). \tag{D.3}$$

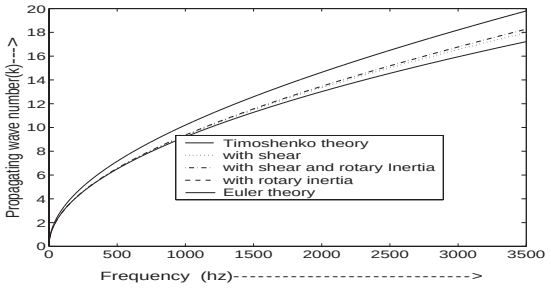

Fig. 23. Variation of propagating wavenumber (k_1) with frequency for various configurations (Timoshenko theory, Timoshenko theory with only transverse shear (third term from last term in Eq. (E.1)), Timoshenko theory with both transverse shear and rotary inertia (second and third terms from last term in Eq. (E.1)) and Euler theory).

Here

$$k_1 = C\omega_1^{1/2}\left(1 - \tfrac{1}{4}\mathrm{i}\eta\right) k_2 = C\omega_2^{1/2}\left(1 - \tfrac{1}{4}\mathrm{i}\eta\right). \tag{D.4}$$

Appendix E

We can write a differential equation for Timoshenko beam theory as follows [1,31]:

$$\frac{B}{\varrho s}\frac{\mathrm{d}^4 w}{\mathrm{d}x^4} + \frac{\mathrm{d}^2 w}{\mathrm{d}t^2} - \left[\frac{I}{s} + \frac{B}{k_f GS}\right]\frac{\mathrm{d}^4 w}{\mathrm{d}x^2\,\mathrm{d}t^2} + \frac{I\varrho}{k_f GS}\frac{\mathrm{d}^4 w}{\mathrm{d}t^4} = 0. \tag{E.1}$$

Eq. (E.1) is very useful to explain difference between Euler theory and Timoshenko theory. Timoshenko theory being a refinement over Euler theory, three additional terms appear which are not present in Euler theory. They are the last three terms in the equation. And they denote, respectively, the effects of rotary inertia, the transverse shear and a coupling term between the two.

Fig. 23 shows a plot of the wavenumber as a function of the frequency (the dispersion curve). The effects of each of the terms mentioned earlier can be seen in the dispersion curve. Each term raises the wavenumber curve over and above that of the Euler curve. Yet, the maximum effect is that of the coupling term. Looking at the total Timoshenko dispersion curve, a given value of the wavenumber k occurs at a frequency lower than that for Euler theory. Thus, the same wavelength occurs at a lower frequency which implies that resonances are lower for Timoshenko theory and the influences are in proportion to the effects of the three terms on the dispersion curve.

References

[1] L. Brillouin, *Wave Propagation in Periodic Structures*, Dover Publications, New York, 1946.
[2] L. Cremer, M. Heckl, *Structure-Borne Sound*, Springer, Berlin, 1973.
[3] G. Sen Gupta, Natural flexural normal modes of periodically-supported finite beams, *Journal of Applied Mechanics* 13 (1950) 89–101.
[4] L. Cremer, Leilich, Zur Theorie der Biegekettenleiter, *Archiv der elektrischen Übertragung* 7 (1953) 261–270.
[5] J.P. Ellington, H. McCallion, Free vibration of grillages, *Journal of Applied Mechanics* 26 (1959) 603–607.

[6] Thein Wah, Natural frequencies of uniform grillages, *Journal of Applied Mechanics* 30 (1963) 571–578.
[7] Thein Wah, Free lateral oscillations of a supported grillage, *Journal of the Franklin Institute* 277 (4) (1964) 349–360.
[8] M. Heckl, Investigations on the vibrations of grillages and other simple beam structures, *Journal of Acoustical Society of America* 36 (7) (1964) 1335–1343.
[9] Y. Yong, Y.K. Lin, Propagation of decaying waves in periodic and piecewise structures of finite length, *Journal of Sound and Vibration* 129 (2) (1989) 99–118.
[10] Y. Yong, Y.K. Lin, Dynamic response analysis of truss-type structural networks, *Journal of Sound and Vibration* 156 (1) (1992) 27–45.
[11] A.H. von Flotow, Disturbance propagation in structural networks, *Journal of Sound and Vibration* 106 (3) (1986) 433–450.
[12] A.K. Roy, R. Plunkett, Wave attenuation in periodic structures, *Journal of Sound and Vibration* 104 (3) (1986) 395–410.
[13] E.M. Kerwin Jr., Damping of flexural waves by a constrained viscoelastic layer, *Journal of Acoustical Society of America* 31 (7) (1959) 952–962.
[14] H. Saito, K. Sato, Flexural wave propagation and vibration of laminated rods and beams, *Transactions of American Society of Mechanical Engineers, Journal of Applied Mechanics* 29 (1962) 287–292.
[15] D.J. Mead, S. Markus, The forced vibration of a three-layer, damped sandwich beam with arbitrary boundary conditions, *Journal of Sound and Vibration* 10 (2) (1969) 163–175.
[16] D.J. Mead, S. Markus, Loss factors and resonant frequencies of encastre damped sandwich beams, *Journal of Sound and Vibration* 12 (1) (1970) 99–112.
[17] D.J. Mead, Free wave propagation in periodically supported, infinite beams, *Journal of Sound and Vibration* 11 (1970) 181–197.
[18] E.S. Reddy, A.K. Mallik, Vibration of a two layered ring on periodic radial supports, *Journal of Sound and Vibration* 84 (3) (1982) 417–430.
[19] E.S. Reddy, A.K. Mallik, Vibration of a three-layered ring on periodic radial supports, *American Institute of Aeronautics and Astronautics Journal* 22 (4) (1984) 543–551.
[20] D.J. Mead, Wave propagation and natural modes in periodic systems: mono-coupled systems, *Journal of Sound and Vibration* 40 (1) (1975) 1–18.
[21] D.J. Mead, Wave propagation and natural modes in periodic systems: multi coupled systems with and without damping, *Journal of Sound and Vibration* 40 (1) (1975) 19–39.
[22] G. Sen Gupta, Natural flexural waves and the normal modes of periodically supported beams and plates, *Journal of Sound and Vibration* 13 (1970) 89–101.
[23] D.W. Miller, A.H. Von Flotow, A travelling wave approach to power flow in structural networks, *Journal of Sound and Vibration* 128 (1) (1989) 145–162.
[24] S. He, M.D. Rao, Vibration and damping analysis of multi span sandwich beams with arbitrary boundary conditions, *Journal of Sound and Vibration* 164 (1) (1993) 125–142.
[25] M. Mace, Damping of beam vibrations by means of a thin constrained visco-elastic layer: evaluation of a new theory, *Journal of Sound and Vibration* 172 (5) (1994) 577–591.
[26] A. Bhimaraddi, Sandwich beam theory and analysis of constrained layer damping, *Journal of Sound and Vibration* 179 (4) (1995) 591–602.
[27] J.E. Bondaryk, Vibration of truss structures, *Journal of the Acoustical Society of America* 102 (4) (1997) 2167–2182.
[28] A. Fasana, S. Marchesiello, Rayleigh–Ritz analysis of sandwich beams, *Journal of Sound and Vibration* 241 (4) (2001) 643–652.
[29] M.B. Xu, L. Huang, Control of multi-span beam vibration by a random wave reflector, *Journal of Sound and Vibration* 250 (4) (2002) 591–608.
[30] M. Junger, D. Feit, *Sound Structures and their Interaction*, Springer, Berlin, 1973.
[31] D.J. Mead, A new method of analyzing wave propagation in periodic structures; applications to periodic Timoshenko beams and stiffened plates. A wave propagation approach, *Journal of Sound and Vibration* 104 (1) (1986) 9–27.
[32] D.G. Crighton, A.P. Dowling, J.E. Ffowcs Williams, M. Heckl, F.G. Leppington, *Modern Methods in Analytical Acoustics*, Springer, Berlin, 1992.